Automatic Classification of Field Winding Faults in Synchronous Motors based on Bicoherence Image Segmentation and Higher Order Statistics of Stray Flux Signals

Miguel E. Iglesias-Martínez, Jose Guerra Carmenate, Jose A. Antonino Daviu , *Senior Member*, *IEEE*, Larisa Dunai , *Member*, *IEEE*, Carlos A. Platero, *Senior Member*, *IEEE*, J. Alberto Conejero, and Pedro Fernández de Córdoba

***Abstract*— In this work, the application of the bicoherence (a squared normalized version of the bispectrum) of the stray flux signal is proposed as a way of detecting faults in the field winding of synchronous motors. These signals are analyzed both under the starting and at steady state regime. Likewise, two quantitative indicators are proposed, the first one based on the maximum values of the asymmetry and the kurtosis of the bicoherence matrix obtained from the flux signals and the second one relying on an algorithm based on the bicoherence image segmentation of the obtained pattern for each analyzed state. The results are analyzed through a comparative study for the two considered motor regimes, obtaining satisfactory results that sustain the potential application of the proposed methodology for the automatic field winding fault detection in real applications.**

***Index Terms*— Bicoherence, Motors, Skewness-Kurtosis, Flux, Winding Faults**

I. Introduction

Condition monitoring of electric motors is of crucial importance in the industry due to the primordial role of these machines that can drive a huge variety of loads in a vast range of different applications. Faults in the electric motors can yield unplanned production downtimes, costly repairs and even user safety hazards. This is the reason why it becomes crucial to develop techniques that are able to reliably detect possible failures or defects in the different components of the electric motor when these failures are still at their early stages of development in the machine [1]-[2].

Wound field synchronous motors (WFSM) are far less widespread in industry than other types of electric motors, such as cage induction motors This is due to the inherent drawbacks that WRSM have, namely: they need auxiliary elements (variable speed drives, damper cages) or machines (pony motors) for their starting, they have more complex constructive characteristics, they have higher cost, etc… [3]. Despite these problems, WFSM can be found in some applications involving high output powers, since they show interesting features at those power ranges, such as higher efficiencies and possibility of power factor regulation [4-5]. Due to this, it is not so unusual to find WFSM rated several MW that operate in certain plants, where they often are critical assets. An interesting case of a catastrophic failure in one of these machines, that implied losses of several million $ is reported in [6].

One of the failures that can happen in WFSM and that can lead to very negative repercussions is the fault in the field winding of these machines. This may happen due to the deterioration of the insulation between field winding turns (caused by a diversity of reasons) which can progress to more severe failures and even to the forced outage of the machine [7].

In this sense several works have been carried out using stray flux signals for this purpose [8-12], then specifically using wound field synchronous motors [13-14]. Despite the variety of works that have analyzed this problem, some issues still remain as the need of expertness of the user that interprets the results of some of the proposed methods, a fact that complicates their implementation in autonomous condition monitoring devices that can be applied in the field.

This work proposes the analysis of stray flux signals both

Miguel E. Iglesias Martínez's work was supported by the postdoctoral research scholarship "Ayudas para la recualificación del sistema universitario español 2021-2023. Modalidad: Margarita Salas", UPV, Ministerio de Universidades, Plan de Recuperación, Transformación y Resiliencia, Spain. Funded by the European Union-Next Generation EU. This work is also supported by Generalitat Valenciana (reference CIAICO/2021/020)

Miguel Enrique Iglesias Martínez is with InterTech Interdisciplinary Modeling Group from the Instituto Universitario de Matemática Pura y Aplicada, Universitat Politècnica de València (UPV), E-46022 Valencia, Spain (e-mail: miigmar@upv.es) and with Grupo de Ingeniería Física, Escuela de Ingeniería Aeronáutica y del Espacio, Universidad de Vigo, Edif. Manuel Martínez Risco, 32004 Ourense. Spain. (email: miguel.iglesias.martinez@uvigo.es)

Jose Guerra Carmenate is with the Departamento de Telecomunicaciones, Universidad de Pinar del Río Hermanos Saíz Montes de Oca, Pinar del Río 20100, Cuba (josegueracarmenate@gmail.com).

Jose A. Antonino-Daviu is with the Instituto Tecnológico de la Energía, Universitat Politècnica de València, E-46022 Valencia, Spain (e-mail: joanda@die.upv.es).

Larisa Dunai is with the Centro de Investigación en Tecnologías Gráficas Universitat Politècnica deValència, E-46022Valencia, Spain (e-mail: ladu@upv.es).

Carlos Platero is with Universidad Politécnica de Madrid, Calle de José Gutierrez Abascal, nº 2, 28006 Madrid, Spain. (carlosantonio.platero@upm.es)

Pedro Fernández de Córdoba is with the Instituto Universitario de Matemática Pura y Aplicada, Universitat Politècnica de València, E-46022 Valencia, Spain (e-mail: pfernandez@mat.upv.es).

under starting and at steady-state for the detection of field winding faults in WFSM. To this end, two high-order statistical analysis using bicoherence are evaluated through the combined application of the skewness and kurtosis indicator. While the bicoherence enables to obtain a visual qualitative representation of the frequency content of the analyzed signals. The second analysis, based on skewness and kurtosis indicator, enables the quantitative discrimination between different fault conditions.

Moreover, the methodology proposes in this paper enables an automatic application of the methodology which is crucial for its possible implementation in autonomous devices. The results included in the paper, which represent an incremental advance versus those presented in [15], show the potential of the approach and its suitability for making the diagnostic user-independent and facilitating its possible future extrapolation to the field.

In synthesis, the main contributions of this work can be listed as follows:

- Proposal of a new methodology for the detection of field winding faults based on stray flux data analysis; the method relies on high order spectral analysis for the calculation of the bicoherence. The method enables an easy qualitative detection of the fault, since it is based on visual patterns.
- Proposal of indicators to quantify the severity of the motor fault using the combination of the kurtosis and the skewness of the flux signal. The indicator is verified in different regimes, proving its usefulness for the determination of the fault severity.
- Proposal of an automatic fault detection scheme based on the segmentation of the image contour obtained from the bicoherence calculation. This scheme makes the method suitable for potential incorporation of the method in automatic condition monitoring systems.

The paper is organized as follows: Section II shows the basic fundamentals of the analysis based on bicoherence. In Section III the experimental details are shown. In Sections IV and V, respectively, the obtained results using bicoherence and the proposed algorithm based on the image segmentation are illustrated. Finally, the conclusions of the work are detailed in Section VI.

II. Theoretical Foundations: Bicoherence Analysis

Higher order spectral analysis is based on the Fourier Transform $X(f)$ of the higher order cumulants of a discrete sequence $\{x(n)\}_{n=0}^{N-1}$ and it can be expressed as follows (where $X(f)$ is the Fourier Transform of the sequence $\{x(n)\}_{n=0}^{N-1}$) [16]-[17]:

$$B(f_1,f_2)=\sum_{\tau_1=1}^{N}\sum_{\tau_2=1}^{N}C_{3x}(\tau_1,\tau_2)\cdot e^{-2\pi f_1\tau_1}\cdot e^{-2\pi f_2\tau_2}$$

$$=\frac{1}{N^2}X(f_1,f_2)\cdot X(f_1)\cdot X(f_2) \qquad (1)$$

In this work, the bispectrum absolute value of the stray flux signal is employed. The discrete theoretical description is given by (2), where *N* is the number of rows of the square matrix *(NxN)* obtained from the bispectrum. The obtained result is a *NxN* matrix that contains the frequency values of the amplitude bispectrum matrix of the analysed stray flux signal [15].

$$(B_x^N(f))=|B_x^N(f_1,f_2)|_i \;\; \forall i=1,\dots,N \qquad (2)$$

On the other hand, the bicoherence can be interpreted as an automatic index that can be calculated from a single signal. It takes values between 0 and 1, which makes it a convenient measure to quantify the degree of phase coupling in a signal. Then, the Bicoherence, according to equation (2), is defined by (3), where the numerator contains the square magnitude of the bispectrum in all segments of the time series and the denominator is the factor that normalizes the bispectrum. Hence, $0 \le B(f_1,f_2) \le 1$.

$$bic^2(f_1,f_2)=\frac{|B(f_1,f_2)|^2}{E\{|X(f_1)X(f_2)|^2\}E\{|X^*(f_1+f_2)|^2\}} \qquad (3)$$

To verify the validity of the theoretical proposal, several experiments are carried out, the results of which are shown below in section IV.

III. Experiments

Different tests were developed using a 4-pole, 400 V WFSM rated 3.4 kVA. The motor was started through a 3-phase variable voltage source. The motor was started thanks to the rotor that assumed the function of the damper, enabling an asynchronous mode starting. The load was an induction motor that acted as generator. A picture of the experimental test bench is shown in Fig.1.

The inter-turn failure was forced by using a variable resistance R_F that could be inserted in parallel at the connections between the poles that can be externally accessed (see Fig.2). The three tested cases were: healthy machine (no resistor connected, i.e., $R_F = \infty$), partial interturn fault in one pole (connected resistor R_F=2.7 **Ω**) and complete short-circuited pole (connected resistor R_F=0 **Ω**).

The stray-flux signals both under the starting and at steady-state were captured using a coil sensor with air core with N1=1000 turns and round shape. It had an external diameter of 80mm and an internal diameter of 39mm (see Fig. 2).

Fig. 1. Experimental testbench.

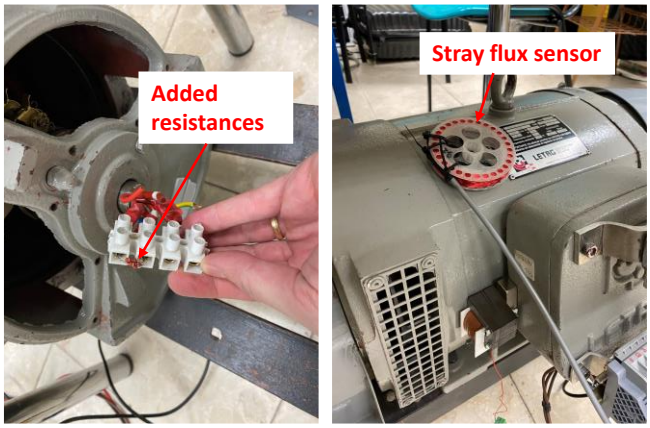

Fig. 2. Inserted resistor to simulate the field winding fault and stray flux sensor used.

IV. Results using Bicoherence Analysis

A. Bicoherence plots.

Sometimes the use of classic signal processing techniques such as the FFT does not constitute an accurate indicator to visually identify a pattern related to the failure in the motor, since the harmonics can be found overlapping with other non-fault related harmonics or even with the spectral noise. An example is depicted in Fig. 3, in which the spectra of the stray-flux signals corresponding to both motor in healthy state, motor with moderate field winding failure and motor with severe field winding failure are shown. Note that a change in the spectral frequencies pattern linked with the winding failure is not clearly observable. Due to this, more sophisticated tools as the bicoherence are proposed in this paper, as a tool to visually enhance the detection of the failure.

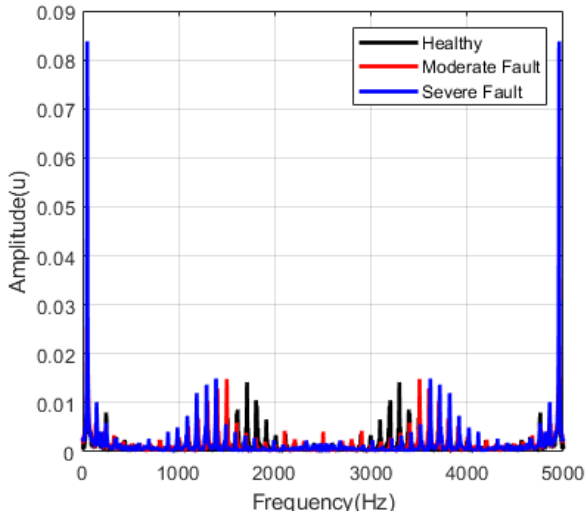

Fig. 3. Comparison of the frequency spectrum of the stray flux signals for a motor in healthy state (black), moderate field winding failure (red) and severe field winding failure (blue)

The following figures show the contour plots corresponding to the bicoherence of the stray flux signals captured under starting and at steady-state operation. In Fig. 4 (healthy condition), no clear pattern can be observed in the upper and lower corners either at steady state or under starting. Note also that at steady state (Fig. 4 (b)) a slight circular pattern appears in the center, around the central frequencies, which is not observed under starting (Fig. 4(a)).

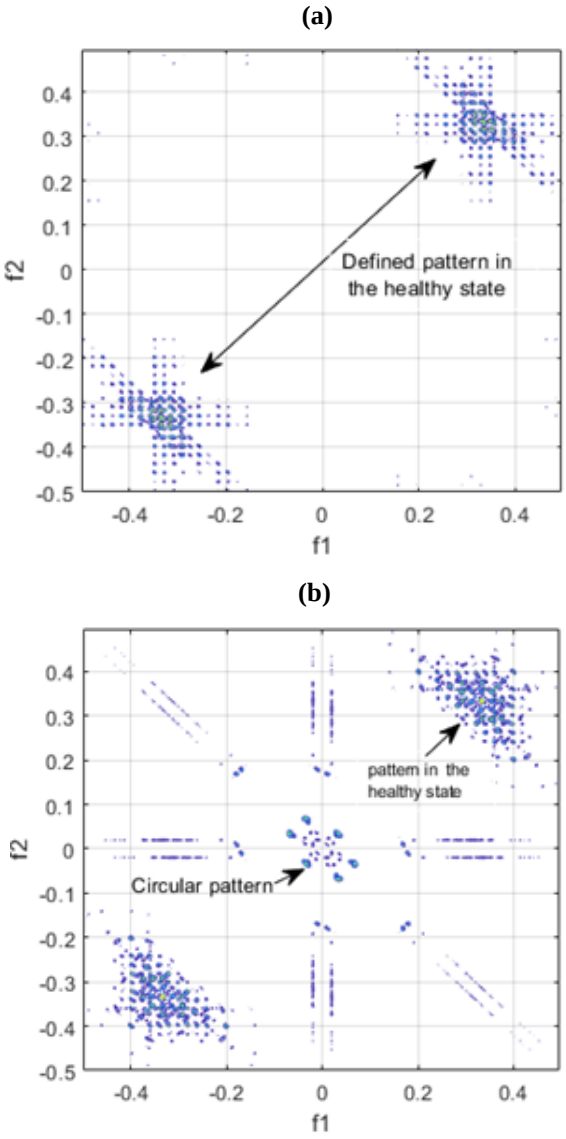

Fig. 4. Bicoherence for healthy condition: (a) under starting, (b) at steady-state

On the other hand, in Fig. 5 (moderate fault level) the bicoherence patterns are different compared to the healthy case. The patterns on the corner are not so concentrated and they spread showing a triangular pattern that expands from the corner, both for the starting (Fig.5 (a)) and for the steady-state (Fig. 5(b)) regimes. Moreover, there is a clear circular pattern in the middle of the contour plot at steady-state regime (Fig. 5 (b)). Finally, Fig. 6 (severe field winding fault level) shows that, as the level of fault worsens, the triangular patterns are even wider for both regimes, while the circular pattern in the middle is clearly noticeable.

The triangular patterns appearing in the bicoherence plots of Figs. 4 and 5 are clear signatures of the fault and are explained by the interactions between the fault frequency components that appear when the field winding failure is present. Moreover, the

width of the pattern is linked with the fault severity, as observed in these figures. The detection of these patterns is rather simple and can be carried out by non-expert users. Moreover, they can be detected by automatic pattern recognition algorithms programmed to this end.

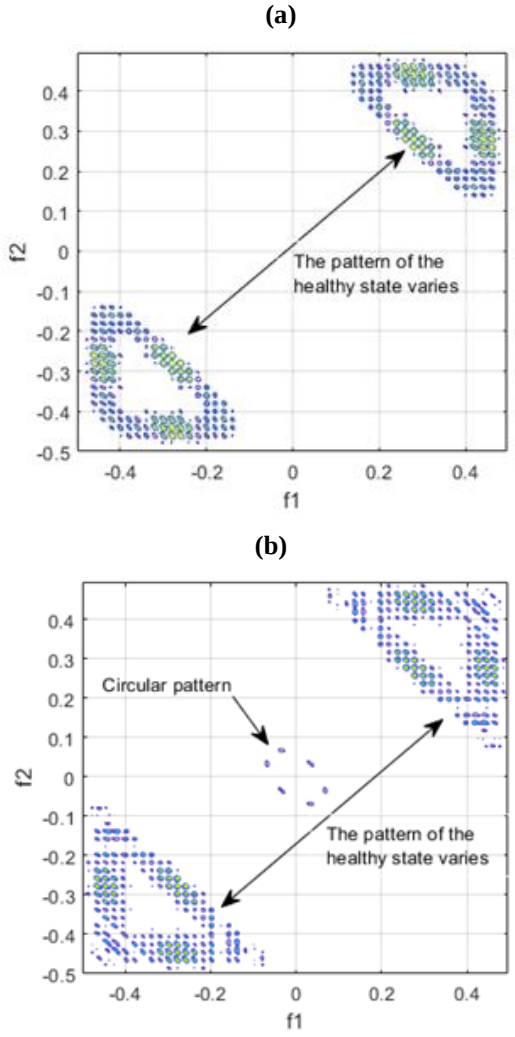

Fig. 5. Bicoherence for the moderate field winding fault condition: (a) under starting, (b) at steady-state.

More specifically, Fig.4 shows a star-shaped pattern that corresponds to the interactions between the frequencies of the harmonics that are already present in healthy condition over the spectrum at steady-state; moreover, a circular pattern can be observed around of 0.1 which indicates the phase coupling with respect to the fundamental frequency. Additionally, there are also replicas of the interactions between multiple harmonics and the fundamental component that yield a circular pattern about 0.2.

In the subsequent figures corresponding to the faulty field winding (Figs. 5 and 6), it can be observed that, at steady state, the external pattern around 0.2 disappears and only the 0.1 pattern around the fundamental frequency remains. On the other hand, there is a residual noise that is only visible when the motor has severe damage. The resulting plots clearly differ from that for healthy condition and allow the detection of the failure.

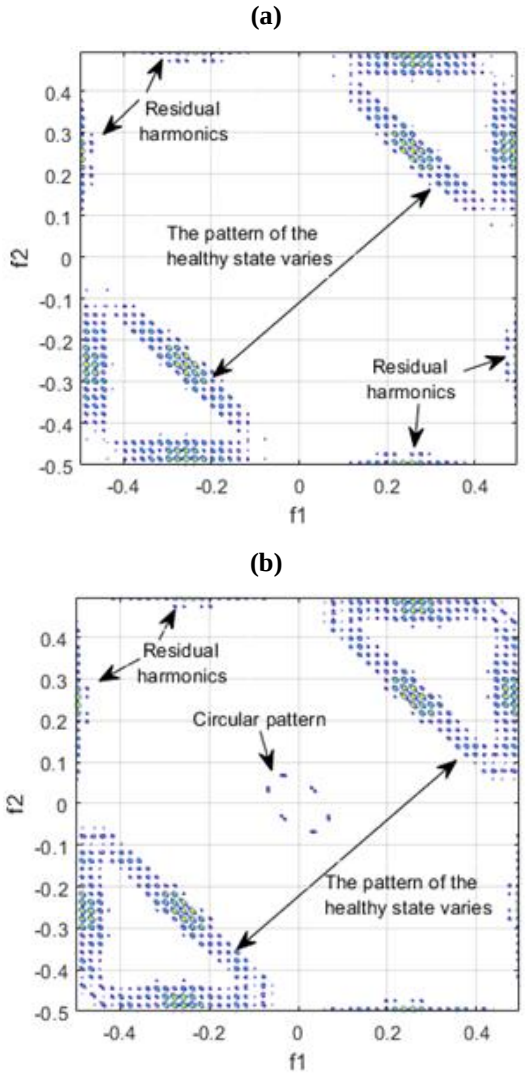

Fig. 6. Bicoherence for the severe field winding fault condition: (a) under starting, (b) at steady-state.

In summary, the proposed method is based, first, on obtaining the bicoherence plots of the healthy machine both during the start-up and at steady-state. In addition, quantitative values of the indicators based on skewness and kurtosis must be computed. Afterwards, during the motor life, the bispectrum plots must be periodically obtained and the fault indicators computed and compared with the healthy ones, detecting deviations that are indicative of the appearance of the fault.

On the other hand, Fig. 7 shows the analysis of the computational cost for evaluating the bicoherence for a data window ranging from 256 samples to 4096 samples. The simulation was carried out on a computer with a W10 12GB of RAM and a third-generation i7 processor. Note that the computational cost rises exponentially as the number of samples to be processed increases. However, also note that the analyses displayed in this paper were performed with only 256 samples of the stray flux signals of the motor in each state, which would imply a computational cost of only 1.3 seconds.

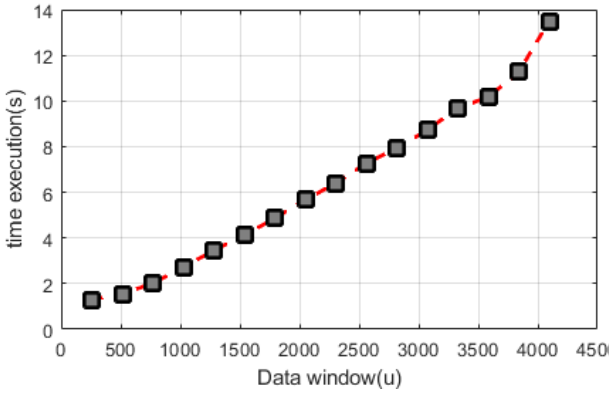

Fig. 7. Computational cost for evaluating the bicoherence for a data window ranging from 256 samples to 4096 samples .

In the following sections, two quantitative indicators are proposed to automatically detect the failure and determine the fault severity. The analyzes were performed both during startup and at steady state.

B. Fault Indicator Based on Skewness and Kurtosis of Bicoherence.

In this work, the use of two fault severity indicators based on high-order statistical analysis, such as asymmetry (S) and kurtosis (k) (see (4)), is proposed. The proposed indicators are based on the maximum values of the asymmetry and the kurtosis of the bicoherence matrix both when the motor is at steady state as well as during startup:

$$S = \frac{E(x-u)^3}{\sigma^3} \qquad k = \frac{E(x-u)^4}{\sigma^4} \tag{4}$$

Then the respective indicators are given by (5), where u is the mean of the *bicoherence*, σ is its standard deviation, and $E(t)$ represents the expected value of the t quantity:

$$Ind_S = \max\left(\frac{E(\,bic^2(f_1,f_2)-u)^3}{\sigma^3}\right) \tag{5}$$

$$Ind_k = \max\left(\frac{E(\,bic^2(f_1,f_2)-u)^4}{\sigma^4}\right)$$

Table I and II show the value of the skewness and kurtosis-based indicators, respectively, revealing a progressive decrement under starting as the winding fault worsens. The trend of both indicators during startup follows a common decreasing pattern, then in steady state it follows an erratic trend. In any case, both fault indicators clearly differ between healthy and faulty conditions, becoming interesting informational sources for the quantification of the fault severity. The difference in the values of the method based on kurtosis reveals a greater range of fault indication, both during start-up and at steady-state, although in the latter the trend is more erratic.

TABLE I. TABLE I. VALUE OF THE SKEWNESS INDICATOR FOR DIFFERENT FAULT CONDITIONS

Under starting		
Healthy	***Moderate fault***	***Severe fault***
8.7227	7.1297	7.0359
At steady-state		
Healthy	***Moderate fault***	***Severe fault***
9.6385	8.2746	9.1977

TABLE II. TABLE II. VALUE OF THE KURTOSIS INDICATOR FOR DIFFERENT FAULT CONDITIONS

Under starting		
Healthy	***Moderate fault***	***Severe fault***
88.8614	61.8200	54.7955
At steady-state		
Healthy	***Moderate fault***	***Severe fault***
102.6651	75.1721	94.1826

Other experiments can be carried out using other types of quantities such as vibrations or acoustic signals of the motor to extend the results obtained. The generalization of the method only implies obtaining a pattern of the healthy state of the motor at the beginning, during start-up and at steady-state, which can be carried out during motor commissioning.

V. BICOHERENCE IMAGE SEGMENTATION

This section is intended to deepen in the automatic fault diagnosis, by applying an image processing methodology to the bicoherence plots obtained in previous sections for each fault condition and considered regime (see Figs. 4 to 6). Based on this method, a second fault indicator is proposed.

In the bicoherence plots of Figs. 4 to 6, a triangular pattern that enabled to detect the fault condition was identified. This pattern varies as the failure increases, but there is a certain graphic similarity in all the triangular obtained patterns.

In order to obtain a function that defines the degree of motor fault as a function of the relative changes of the bicoherence pattern, an algorithm based primarily on binary segmentation using the Otsu method [18] to filter the relevant information is proposed. Once a clean pattern is obtained, the information is processed. Otsu's method is a variance-based technique to find the threshold value where the weighted variance between foreground and background pixels is minimal. The Otsu method [19-20], can be described as follows:

$$K_i = \frac{\sigma^2 B}{\sigma^2 G} \tag{6}$$

where K_i is the threshold value, $\sigma^2 B$ is a global variance of the entire image and $\sigma^2 G$ is the variance between classes. Once

every image is segmented, to process the information, three fixed-size quadrants are extracted from all the images; hence, there is a total of nine quadrants, corresponding to the bicoherence during startup and at steady-state for each condition (healthy, moderate and severe failure). Fig. 7 and 8 show, respectively, the results of this segmentation process.

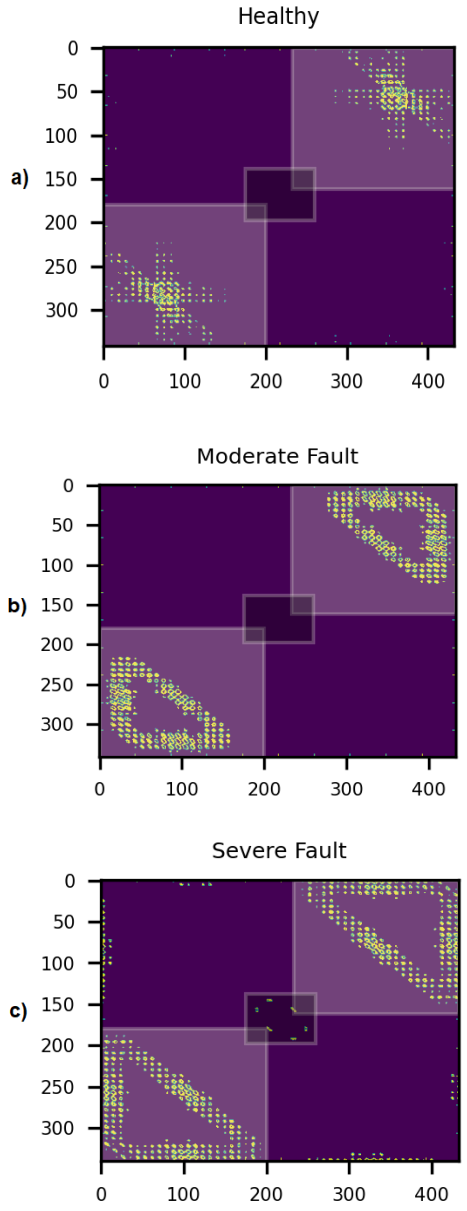

Fig. 8. Bicoherence image segmentation during startup. a) Healthy b) Moderate Fault c) Severe Fault.

The three selected regions for each picture are: the upper right and lower left corners, representing the variation of the triangular patterns, and the center region that is the one that differentiates between the starting and the steady state.

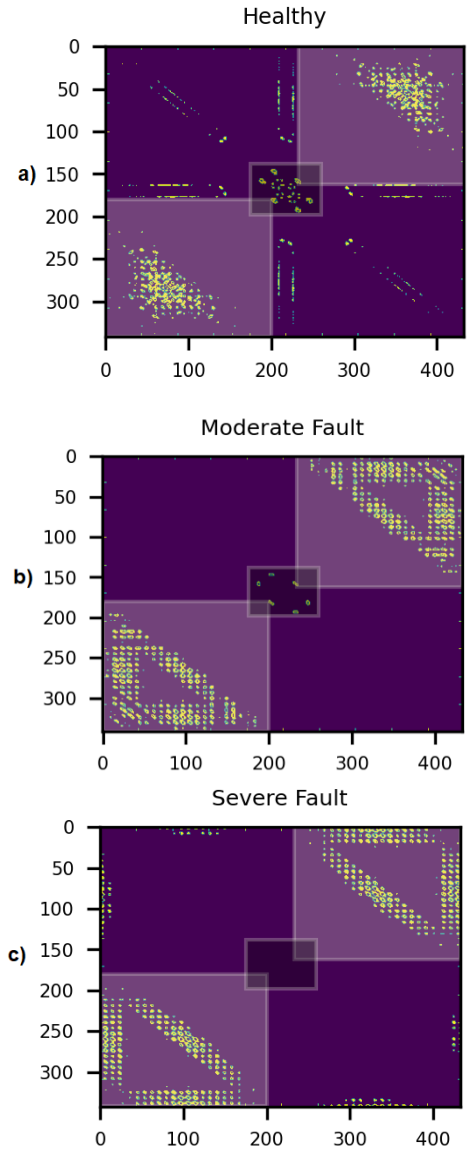

Fig. 9. Bicoherence image segmentation at steady state. a) Healthy b) Moderate Fault c) Severe Fault.

In the previous figures it can be noticed that, unlike what happens at steady state, the circular pattern of harmonics does not appear during the startup. Once the segmentation is obtained, an analysis of the pixels "on/off" is carried out in each quadrant. The relationship is represented as follows:

$$F(e,a) = P(x,y) \quad \nabla\ x,y\ \in\ \mathbb{R} \tag{7}$$

where $P(x,y)$ is the point that represents the relation in a plane.

A. Function to evaluate the fault severity

Once the segmentation is obtained, a fault indicator function is proposed. It is based on spiraling through a matrix of fixed size that contains the relevant information of each one of the selected quadrants.

If the patterns obtained in Figs. 7 and 8 are analyzed, it can be noticed that, as the fault becomes more severe, a triangular-shaped area of "off" pixels in the center of the pattern (figures

7b, 7c, 8b, 8c) is generated. When the fault increases, the "on" pixels are very close to the edges, due to the increase in the triangular area (Figs.7c and 8c respectively). On the contrary, in the healthy case, there is a pattern of "on" pixels concentrated close to the quadrant center. The idea is to weight with a greater value those pixels that are closer to the edges, since the underlying hypothesis is that the edges are related to the fault while the center to the healthy state.

Based on these ideas, three quadrants are taken in each image for the three considered conditions (see Figs 7 and 8); the central quadrant is taken to discriminate between the START-UP regime and the STEADY-STATE, while the UPPER RIGHT and LOWER LEFT quadrants are used to assess the severity of the motor failure.

The main idea of the proposed algorithm is to run through each quadrant following a spiral of the NxN quadrant matrix; in this way, the farthest layer from the center is run in each iteration (Fig. 10).

A weight with value 100 is initialized and it will decrease 10% of its current value in each iteration, in such a way that the weight is maximum in iteration 1 (closer to the edge) and minimum in the last iteration (closer to the center). The matrix iteration process is shown in Fig. 10.

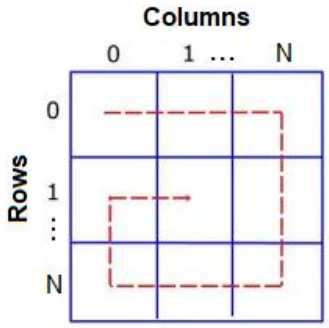

Fig. 10. Spiral matrix algorithm for fault indicator function.

The function takes an array as an input, that corresponds to the quadrant to be analyzed. Starting from a null value, $Failure = 0$ and using the following operation variables:

- $max_x \rightarrow$ X matrix Dimension (quadrant)
- $max_y \rightarrow$ Y matrix Dimension (quadrant)
- $aux_x \rightarrow$ iteration of the matrix by the X dimension
- $aux_y \rightarrow$ iteration of the matrix by the Y dimension
- $weigth \rightarrow$ Pixel Weight

A flowchart description of the functionality of the proposed method that yields an indicator of the severity of motor fault is shown in Fig. 11, 12 and 13 respectively.

The first step of the iteration process is to calculate the upper quadrant region of the matrix obtained from the contour representation of the bicoherence (see Figs. 8 and 9, respectively).

Subsequently, the regions of the right and lower quadrant are calculated, and finally the region of the left quadrant. Each iteration is performed taking into account the variables listed above.

The updating process of each loop is executed until reaching the matrix dimensions, represented by the max_x y max_y variables respectively. Before the completion of the first iteration of the general loop, all auxiliary variables represented by aux_x , aux_y are updated. These variables correspond to the iteration index for the X and Y quadrant dimension, respectively.

Finally, the cumulative sum of the weights represented by each pixel, which in this case corresponds to the variable $weigth$, is updated. This cumulative sum corresponds to the weights of the pixels of the matrix of each quadrant, for each motor condition.

The whole process is repeated from step 1 to step 3 until the analysis of all graphical information provided by the segmentation of the bicoherence contour image is covered.

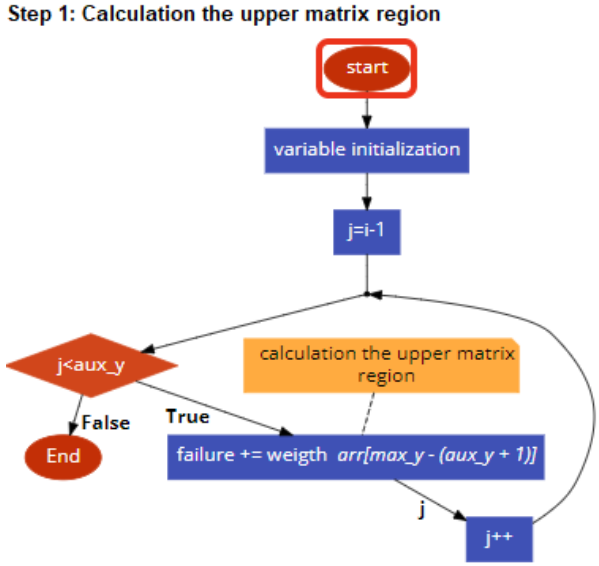

Fig. 11. Ilustration of: Step 1 of the flowchart description of the functionality of the proposed method based on bicoherence image segmentation.

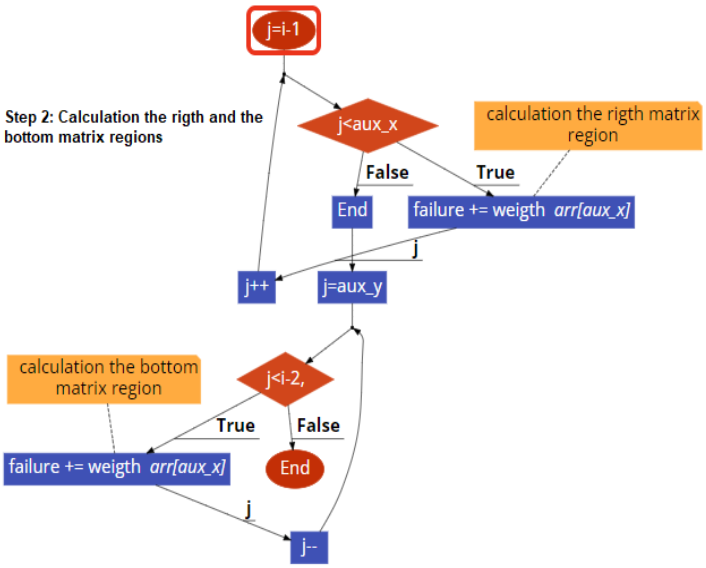

Fig. 12. Ilustration of : Step 2 of the flowchart description of the functionality of the proposed method based on bicoherence image segmentation.

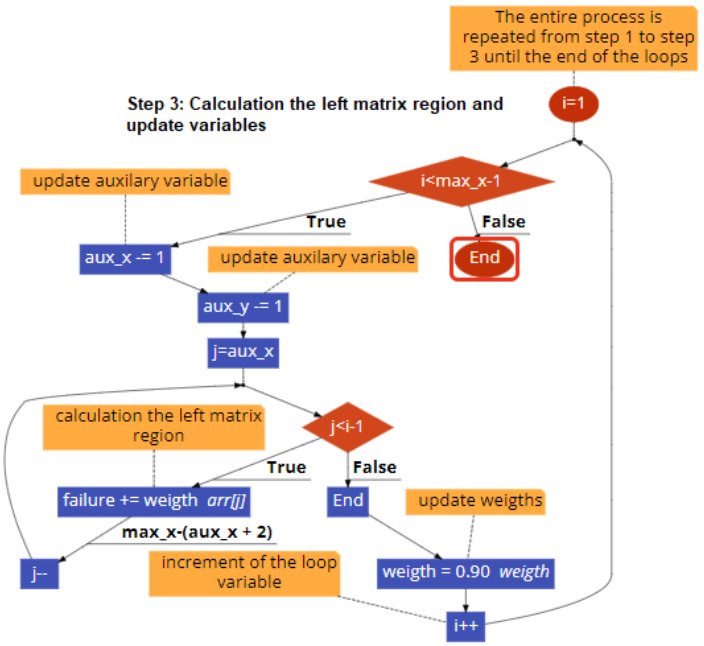

Fig. 13. Ilustration of: Step 3 of the flowchart description of the functionality of the proposed method based on bicoherence image segmentation.

As a result of the application of the proposed algorithm, a non-dimensional indicator is obtained that facilitates to determine the fault severity; this indicator increases its value as the severity of the failure gets worse. The results can be observed in Fig. 14, in which an upward trend can be observed for both considered regimes (i.e. the startup and the steady state), as the fault severity increases.

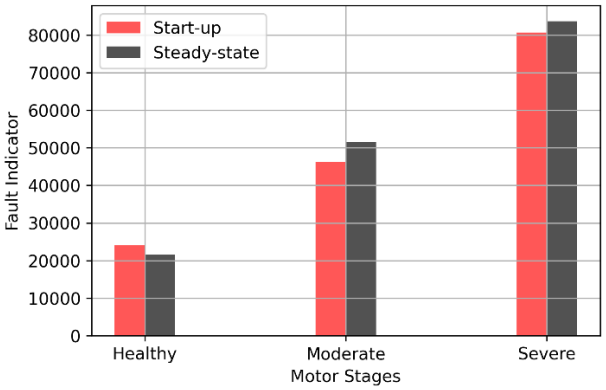

Fig. 14. Output and trend of the fault indicator function based on bicoherence image segmentation.

VI. Conclusion

This work has proposed a field winding fault detection method for WFSM based on the bicoherence analysis of stray flux signals. In the paper, the potential of the use of high-order spectral analysis and its combination with statistical indicators based on cumulants such as asymmetry and kurtosis is assessed. Two methodologies for different regimes (starting and steady-state) are applied.

On the other hand, a fault indicator function based on the segmentation of the image patterns obtained from bicoherence is also proposed. The method is based on segmenting the area of relevant information and developing a spiral matrix processing algorithm to obtain a quantitative indicator of the fault severity.

Under both regimes, it is possible to discern, by using the bicoherence image pattern whether the motor is healthy, or it has a certain level of field winding failure. Likewise, it is shown that the indicators calculated based on higher order central cumulants as skewness and kurtosis are also a good alternative to determine the fault severity, showing better results under starting.

Finally, the results of this work can be generalized and incorporated into real time motor condition monitoring systems. The use of high order statistics offers the possibility of detecting other types of faults given the noise immunity of high order spectral analysis techniques. This can be an interesting tool to explore the detection of other types of faults in synchronous motors as well as to apply the method to other machines, as induction motors.

References

[1] Abid, A., Khan, M.T. & Iqbal, J. A review on fault detection and diagnosis techniques: basics and beyond. Artif Intell Rev 54, 3639–3664 (2021).

[2] Gundewar, S.K., Kane, P.V. Condition Monitoring and Fault Diagnosis of Induction Motor. J. Vib. Eng. Technol. 9, 643–674 (2021).

[3] Zamudio-Ramirez, R. A. A. Osornio-Rios, J. A. Antonino-Daviu, H. Razik and R. d. J. Romero-Troncoso, "Magnetic Flux Analysis for the Condition Monitoring of Electric Machines: A Review," in IEEE Transactions on Industrial Informatics, doi: 10.1109/TII.2021.3070581.

[4] J. Shin, Y. Park and S. B. Lee, "Flux-Based Detection and Classification of Induction Motor Eccentricity, Rotor Cage, and Load Defects," in IEEE Transactions on Industry Applications, vol. 57, no. 3, pp. 2471-2480, May-June 2021.

[5] M. E. Iglesias Martínez, J. A. Antonino-Daviu, P. F. de Córdoba, J. A. Conejero and L. Dunai, "Automatic Classification of Winding Asymmetries in Wound Rotor Induction Motors Based on Bicoherence and Fuzzy C-Means Algorithms of Stray Flux Signals," in IEEE Transactions on Industry Applications, vol. 57, no. 6, pp. 5876-5886, Nov.-Dec. 2021.

[6] J. Antonino-Daviu. V. Fuster-Roig, S. Park, Y. Park, H. Choi, J. Park and S.B. Lee, "Electrical Monitoring of Damper Bar Condition in Salient-Pole Synchronous Motors Without Motor Disassembly," in IEEE Transactions on Industry Applications, vol. 56, no. 2, pp. 1423-1431, Mar-Apr 2020.

[7] J. Yun, S. B. Lee, M. Šašić and G. C. Stone, "Reliable Flux-Based Detection of Field Winding Failures for Salient Pole Synchronous Generators," in IEEE Transactions on Energy Conversion, vol. 34, no. 3, pp. 1715-1718, Sept. 2019.

[8] L. Frosini, “Novel diagnostic techniques for rotating electrical machines -A review”, in Energies, 2020, 13(19), 5066, https://doi.org/10.3390/en13195066

[9] K. N. Gyftakis, P. A. Panagiotou and S. B. Lee, "Generation of Mechanical Frequency Related Harmonics in the Stray Flux Spectra of Induction Motors Suffering From Rotor Electrical Faults," in IEEE Transactions on Industry Applications, vol. 56, no. 5, pp. 4796-4803, Sept.-Oct. 2020, doi: 10.1109/TIA.2020.3002975.

[10] X. Wang et al., "Stray Flux-Based Rotation Angle Measurement for Bearing Fault Diagnosis in Variable-Speed BLDC Motors," in IEEE Transactions on Energy Conversion, vol. 36, no. 4, pp. 3156-3166, Dec. 2021, doi: 10.1109/TEC.2021.3079444.

[11] Garcia-Calva T, Morinigo-Sotelo D, Fernandez-Cavero V, Romero-Troncoso R. Early Detection of Faults in Induction Motors A Review. Energies. 2022; 15(21):7855. https://doi.org/10.3390/en15217855

[12] F. J. M. Dias, G. G. Sotelo and R. d. A. Júnior, "Performance Comparison of Superconducting Machines With Induction Motors," in IEEE

Transactions on Applied Superconductivity, vol. 32, no. 7, pp. 1-5, Oct. 2022, Art no. 5202805, doi: 10.1109/TASC.2022.3188461.

[13] M. F. Shaikh, J. Park, Y. Park, S. B. Lee and J. A. Antonino-Daviu, "Electrical Testing for Detection and Classification of Open Damper Bar and Shorted Field Winding Failures in Wound Field Synchronous Motors," in IEEE Transactions on Industry Applications, vol. 58, no. 4, pp. 4532-4541, July-Aug. 2022, doi: 10.1109/TIA.2022.3167017.

[14] K. N. Gyftakis, C. A. Platero and J. K. Nøland, "Multi-Parametric Monitoring of Medium-Power Generators with Brushless Exciters under Mechanical Faults," 2022 International Conference on Electrical Machines (ICEM), Valencia, Spain, 2022, pp. 1524-1529, doi: 10.1109/ICEM51905.2022.9910891.

[15] J. G. Carmenate et al., "Bicoherence and Skewness-Kurtosis Analysis for the Detection of Field Winding Faults in Synchronous Motors using stray flux signals," 2022 IEEE Energy Conversion Congress and Exposition (ECCE), 2022, pp. 1-5

[16] M. E. Iglesias-Martínez, P. Fernández de Córdoba, J. A. Antonino-Daviu and J. Alberto Conejero, "Bispectrum Analysis of Stray Flux Signals for the Robust Detection of Winding Asymmetries in Wound Rotor Induction Motors," 2020 IEEE Energy Conversion Congress and Exposition (ECCE), 2020, pp. 4485-4490.

[17] M. E. I. Martínez, J. A. Antonino-Daviu, C. Platero, L. Dunai, J. A. Conejero and P. F. de Cordoba, "Multifractal Spectrum and Higher Order Statistics for the Detection of Field Winding Faults in Wound Field Synchronous Motors," 2021 IEEE 19th International Conference on Industrial Informatics (INDIN), 2021, pp. 1-7.

[18] Otsu, N., "A Threshold Selection Method from Gray-Level Histograms." IEEE Transactions on Systems, Man, and Cybernetics. Vol. 9, No. 1, 1979, pp. 62–66.

[19] W. A. Mustafa, W. Khairunizam, Z. Ibrahim, S. A. B. and Z. M. Razlan, "A Review of Different Segmentation Approach on Non Uniform Images," 2018 International Conference on Computational Approach in Smart Systems Design and Applications (ICASSDA), 2018, pp. 1-6,

[20] Jaiswal, S., Pandey, M.K. (2021). A Review on Image Segmentation. In: Rathore, V.S., Dey, N., Piuri, V., Babo, R., Polkowski, Z., Tavares, J.M.R.S. (eds) Rising Threats in Expert Applications and Solutions. Advances in Intelligent Systems and Computing, vol 1187. Springer, Singapore.

VI. BIOGRAPHIES

Miguel Enrique Iglesias Martínez received a degree in Telecommunications and Electronics Engineering from the University of Pinar del Río (UPR) in 2008 and a Master's Degree in Digital Systems from the Technological University of Havana, Cuba, in 2011. In 2020 he received his doctorate in Mathematics at Universitat Politècnica de València, obtaining best dissertation award in the area of science. He is currently a postdoctoral researcher of the "Margarita Salas" Program, of the Ministry of Universities of the Government of Spain, assigned to the School of Aeronautical and Space Engineering of the University of Vigo. He is also an associate researcher in the Interdisciplinary Modeling Group, InterTech (www.intertech.upv.es) of the University Institute of Pure and Applied Mathematics at the Universitat Politècnica de València. His areas of research interest are signal processing, noise analysis and information extraction, as well as pattern recognition systems.

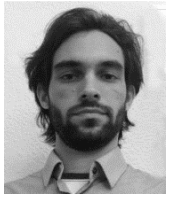

José Guerra Carmenate was born in Pinar del Río Cuba in 1995. He received the B.Sc. degree in telecommunications and electronics engineering from the University of Pinar del Río, Pinar del Río, Cuba, in 2019. Is currently working toward the Ph.D. degree in mathematics at the Universitat Politècnica de València, Valencia, Spain. His research interests include acquisition and analysis of environmental data, design and implementation of IoT sensors, as well as digital signal processing.

Jose Antonino-Daviu (S'04, M'08, SM'12) received his M.S. and Ph. D. degrees in Electrical Engineering, both from the Universitat Politècnica de València, in 2000 and 2006, respectively. He also received his Bs. in Business Administration from Universitat de Valencia in 2012. He was working for IBM during 2 years, being involved in several international projects. Currently, he is Full Professor in the Department of Electrical Engineering of the mentioned University, where he develops his docent and research work. He has been invited professor in Helsinki University of Technology (Finland) in 2005 and 2007, Michigan State University (USA) in 2010, Korea University (Korea) in 2014 and Université Claude Bernard Lyon 1 (France) in 2015. He is IEEE Senior Member since 2012 and he has published over 300 contributions, including international journals, conferences and books. He is also Associate Editor of IEEE transactions on Industrial Informatics, IEEE Industrial Electronics Magazine, IEEE transactions on Sustainable Energy, IEEE transactions on Cybernetics and IEEE Journal of Emerging and Selected Topics in Industrial Electronics. He is also IEEE IAS Prominent Lecturer for 2022-23. He was General Co-Chair of IEEE SDEMPED 2013 and ICEM 2022. He received the Nagamori Award from Nagamori Fundation in Kyoto, Japan in 2018, for his contributions in electric motors transient analysis area. In 2019, he was awarded with the SDEMPED Diagnostic Achievement Award in Toulouse, France.

Larisa Dunai (M´19)**,** Associate Professor at UPV, obtained her MSc degree in Electronic Engineering in 2003 from Technical University of Moldova and a Master degree in Electronic Engineering in 2004 at the same university. After obtaining the MSc degree joined the Technical University of Moldova as Assistant professor at the Radio electronics and Telecommunications Department. In 2007 she started working as a researcher in the Research Center in Graphic Technology (CITG) of the Universidad Politecnica de Valencia. In November 2008 she joined the UPV as an Assistant professor of Graphic Design Department. In 2010 obtained her PhD at Universitat Politècnica de València. In 2013 she received the MIT Innovators Award for Spain and in 2014 the Michael Richey Medal from Royal Institute of Navigation.

Carlos A. Platero (M'10-SM'20) was born in Madrid, Spain, in 1972. He obtained his Dipl. degree and Ph.D. degree in Electrical Engineering from the Universidad Politécnica de Madrid, Spain, in 1996 and 2007 respectively. From 1996 to 2008 he worked in ABB Generación S.A., Alstom Power S.A. and ENDESA Generación SA, and was involved in the design and commissioning of power plants. In 2002 he started teaching at the Electrical Engineering Department of the Universidad Politécnica de Madrid and joined an energy research group. In 2008 he became a full-time Associate Professor.

J. Alberto Conejero received the B.Sc. and M.Sc.degree in mathematics from the Universitat de València, Valencia, Spain, in 1998, the M.Sc. degree in bioinformatics and biostatistics from the Universitat Oberta de Catalunya and the Universitat de Barcelona, Barcelona, Spain, in 2020, and the Ph.D. degree in applied mathematics from the Universitat Politècnica de València (UPV), Valencia, Spain, in 2004, receiving the Outstanding Dissertation Award. Since 2020, he has been a Full Professor with UPV. He is currently the Director of the Department of Applied Mathematics, UPV, and responsible for the M.Sc. program on Mathematics Research with UPV. He has been Visiting Scholar with Bowling Green St. University, USA; Kent St. University, USA; Università del Salento, Italy; Universität Tübingen, Germany; and Czech Academy of Sciences, Czech Republic. His research interests include dynamical systems, partial differential equations, graph theory, network science, and the multidisciplinary applications of mathematics to computer science, engineering, and biotechnology. Dr. Conejero was the recipient of the Teaching Excellence Prize of UPV in 2014, and he won the XPRIZE $500k Pandemic Response Challenge with VALENCIA IA4COVID team in 2021.

Pedro Fernández de Córdoba was born in Valencia in October 1965. He received the B.Sc., M.Sc., and Ph.D. degrees in physics from the Universitat de València (UV), Valencia, Spain, in 1988, 1990, and 1992, respectively. He also received the Ph.D. degree in mathematics from the Universidad Politécnica de Valencia (UPV), Valencia, in 1997. His research work was performed at UV, UPV, the Joint Institute for Nuclear Research (Russia), the University of Tübingen (Germany), and the Istituto Nazionale di Fisica Nucleare, Torino, Italy, among others. He is currently a Professor with the Department of Applied Mathematics, UPV. His research interests include the area of modeling and numerical simulation of physical and engineering problems, mainly focusing on the nu- merical treatment of heat and mass transfer problems. Dr. de Córdoba is Doctor Honoris Causa from the University of Pinar del Rio (Cuba), a member of the Colombian Academy of Exact, Physical and Natural Sciences, a member of the Académie Nationale des Sciences, Arts et Lettres du Bénin, Profesor Invitado of the University of Pinar del Rio, and Profesor Visitante “Ad Honorem” of the Universidad del Magdalena (Colombia). Furthermore, since its establishment on September 30, 2011, he has been a member of the Board of the Spanish Mathematics-Industry network (www.math-in.net).